International Journal of Applied Mathematics
Volume 39 No. 1s, 2026
ISSN: 1311-1728 (printed version); ISSN: 1314-8060 (on-line version)

LYAPUNOV SPECTRUM ANALYSIS AND NUMERICAL CHARACTERISATION OF A NEW FOUR-DIMENSIONAL NONLINEAR SYSTEM

Brahim BENZEGHLI*
*Department of Mathematics, University of Batna 2, Batna, 05000, Algeria.

Abstract

In this work we introduce a new nonlinear autonomous system in four dimensions that includes quadratic interactions and possesses a one-parameter family of equilibrium points. A comprehensive numerical investigation of the Lyapunov spectrum of this system is carried out. To this end, a Benettin–Wolf type algorithm with periodic QR reorthonormalization is implemented to approximate all Lyapunov exponents and the corresponding Kaplan–Yorke dimension.

Over a broad range of parameter values, the system displays chaotic dynamics characterized by a positive largest exponent and an attractor whose effective dimension slightly exceeds two. The reliability of the numerical procedure is assessed by examining its sensitivity to the integration step, the length of the discarded transient, and the renormalization interval. Parameter-dependent plots of the Lyapunov exponents and the Kaplan–Yorke dimension are then used to single out parameter regions where the chaotic behavior is more pronounced. The proposed model and computational routine are finally compared with existing four-dimensional systems and Lyapunov exponent methods, and possible uses in secure communications and image encryption are briefly outlined.

Mathematics Subject Classification 2020: 37D45, 37M22, 37D10, 37C10.

Keywords: Lyapunov exponents, Kaplan–Yorke dimension, four-dimensional nonlinear system, chaotic dynamics, numerical integration, QR method.

1. Introduction

Lyapunov exponents and the associated Lyapunov spectrum are central tools for the quantitative study of nonlinear dynamical systems. They measure average exponential separation or convergence of nearby trajectories and are routinely used to detect and characterise chaotic behaviour [3, 1, 4]. For systems of dimension three or higher, knowledge of the full spectrum yields information about the geometry of attractors and about the number of effectively expanding directions, which can be related to fractal dimensions through the Kaplan–Yorke conjecture [7, 8]. Obtaining accurate and robust numerical estimates of Lyapunov exponents is therefore important both for theoretical investigations and for applications.

Substantial effort has been devoted in recent years to the development and analysis of numerical techniques for Lyapunov exponents, including algorithms based on QR and singular value decompositions, simplified schemes targeting only the largest exponent, and specialised methods for fractional-order, delay, or non-smooth systems [1, 5, 6]. In parallel, many new chaotic and hyperchaotic models have been proposed, particularly in four dimensions,

Received: Aug 08, 2025

International Journal of Applied Mathematics
Volume 39 No. 1s, 2026
ISSN: 1311-1728 (printed version); ISSN: 1314-8060 (on-line version)
motivated by tasks such as secure communication, image encryption, and complex network modelling [9, 10, 11, 12, 13, 14]. For these systems, a dependable computation of the Lyapunov spectrum is a key ingredient in confirming the presence of chaos, estimating attractor dimensions, and comparing the dynamical richness of different models.

The present paper pursues two main objectives. First, it introduces a four-dimensional autonomous system with quadratic nonlinearities and a continuous line of equilibria, and studies its dynamics through qualitative analysis and numerical simulations. The system supports bounded attractors, irregular time series, and multi-scroll structures in phase space for suitable parameter choices. Second, it develops and implements a Benettin–Wolf type numerical routine designed to compute the full Lyapunov spectrum of the model, together with the Kaplan–Yorke dimension. The routine couples a standard fourth-order Runge–Kutta integrator for the base trajectory with the evolution of tangent vectors and periodic QR reorthonormalization, with the aim of providing a simple yet numerically robust tool [17, 3, 4, 15, 16].

The main contributions can be summarised as follows.

- A new four-dimensional nonlinear system with quadratic couplings is defined and analysed; its equilibria and local properties are determined, and it is shown to be dissipative for all parameter values $a > 0$.
- A Benettin–Wolf/QR algorithm tailored to this model is constructed, and a detailed numerical study of the Lyapunov spectrum and Kaplan–Yorke dimension is carried out over a range of parameter values.
- The influence of numerical parameters, such as time step, transient length, and renormalization frequency, on the computed exponents is examined, and the resulting spectra are compared with those of other four-dimensional chaotic systems reported in the literature.

The remainder of the paper is organised as follows. Section 2 recalls the basic definitions of Lyapunov exponents and the Kaplan–Yorke dimension. Section 3 introduces the four-dimensional system, determines its equilibria, and discusses dissipativity. Section 4 presents the numerical routine for computing the Lyapunov spectrum. Section 5 reports numerical results, including time series, phase portraits, convergence tests, and parameter-dependent diagrams. Section 6 compares the routine and the system with existing methods and models, and Section 7 outlines conclusions and possible directions for future work.

2. Preliminaries

This section recalls the notions of Lyapunov exponents and Kaplan–Yorke (Lyapunov) dimension that will be used later, and fixes notation for the numerical algorithms applied to the four-dimensional system [1, 3, 4, 6, 15].

2.1 Lyapunov exponents for continuous-time systems

Consider a smooth autonomous system

$$\dot{x} = f(x), x(t) \in \mathbb{R}^n$$

Received: Aug 08, 2025

International Journal of Applied Mathematics
Volume 39 No. 1s, 2026
ISSN: 1311-1728 (printed version); ISSN: 1314-8060 (on-line version)
where $f \in C^1(\mathbb{R}^n, \mathbb{R}^n)$. For an initial state $x(0) = x_0$, the solution is denoted by $x(t; x_0)$. Infinitesimal perturbations of the initial condition are governed by the variational equation

$$\dot{Y}(t) = Df\big(x(t; x_0)\big)Y(t), Y(0) = Y_0 \qquad (1)$$

where Df is the Jacobian matrix of f and $Y(t)$ is an $n \times n$ matrix that maps initial perturbations to perturbations at time t.

Under standard regularity and ergodicity assumptions, Oseledec's multiplicative ergodic theorem ensures that, for almost every initial condition, there exist real numbers

$$\lambda_1 \geq \lambda_2 \geq \cdots \geq \lambda_n$$

called the (global) Lyapunov exponents, which describe the asymptotic exponential growth rates of typical tangent vectors along the flow. If $Y(t)$ solves the variational equation with $Y(0) = I_n$ and $\sigma_1\big(Y(t)\big) \geq \cdots \geq \sigma_n\big(Y(t)\big)$ denote the singular values of $Y(t)$, one has

$$\lambda_i = \lim_{n\to\infty} \frac{1}{t} \log \sigma_i\big(Y(t)\big), i = 1, \dots, n.$$

A positive Lyapunov exponent indicates exponential divergence of nearby trajectories and is widely used as a quantitative indicator of chaos [3, 1, 16].

In numerical practice, the Lyapunov spectrum is usually approximated by integrating the original system together with a suitable set of tangent vectors and by periodically reorthonormalizing these vectors using a QR-type procedure [1, 4, 2]. This leads to the classical Benettin–Wolf algorithm and its QR-based variants, which will be employed later for the four-dimensional model under study [17, 6].

2.2 Kaplan–Yorke (Lyapunov) dimension

Let

$$\lambda_1 \geq \lambda_2 \geq \cdots \geq \lambda_n$$

be an ordered Lyapunov spectrum. The Kaplan–Yorke (or Lyapunov) dimension D_{KY} associated with the attractor is defined as follows [7, 3]. Let j be the largest integer in $\{0,1, \dots, n-1\}$ such that

$$\lambda_1 + \cdots + \lambda_j \geq 0, \lambda_1 + \cdots + \lambda_{j+1} < 0.$$

Then

$$D_{KY} = j + \frac{\lambda_1 + \cdots + \lambda_j}{|\lambda_{j+1}|} \qquad (2)$$

By convention, if $\lambda_1 < 0$ one sets $D_{KY} = 0$, whereas if $\lambda_1 + \cdots + \lambda_n \geq 0$ one may take $D_{KY} = n$ [7, 8]. The Kaplan–Yorke dimension is widely used as an estimate of the fractal dimension of chaotic attractors and will be used below to quantify the complexity of chaotic and hyperchaotic regimes in the proposed four-dimensional system [9, 10, 11].

2.3 Notation for the 4D system and its spectrum

Received: Aug 08, 2025

International Journal of Applied Mathematics
Volume 39 No. 1s, 2026
ISSN: 1311-1728 (printed version); ISSN: 1314-8060 (on-line version)
The analysis in this paper focuses on a nonlinear autonomous system in four dimensions of the form

$$\dot{x} = f_{a,p}(x), x(t) \in \mathbb{R}^4$$

depending on a positive parameter $a > 0$ and a real parameter $p \in \mathbb{R}$. For each pair (a, p), the Lyapunov spectrum is denoted by

$$\lambda_1(a,p) \geq \lambda_2(a,p) \geq \lambda_3(a,p) \geq \lambda_4(a,p)$$

and the corresponding Kaplan–Yorke dimension by $D_{KY}(a,p)$, defined via the formula above.

Parameter regions where at least two Lyapunov exponents are positive,

$$\lambda_1(a,p) > \lambda_2(a,p) > 0 > \lambda_3(a,p) \geq \lambda_4(a,p)$$

will be referred to as hyperchaotic regimes, in analogy with other four-dimensional hyperchaotic systems discussed in the literature [9, 12, 13].

3. The proposed four-dimensional system

This section introduces the four-dimensional system that will be studied, explains its structural features, and analyses its equilibria, Jacobian, and dissipativity.

3.1 System definition and motivation

Consider the following four-dimensional autonomous system depending on two real parameters $a > 0$ and $p \in \mathbb{R}$:

$$\begin{cases} \dot{x}_1 = a(x_2 - x_1), \\ \dot{x}_2 = x_1(p - x_3) + x_1 x_4, \\ \dot{x}_3 = -x_3 + x_1 x_2, \\ \dot{x}_4 = x_2 x_3, \end{cases} \tag{3}$$

with $x = (x_1, x_2, x_3, x_4)^\top \in \mathbb{R}^4$. The first equation is reminiscent of the Lorenz/Chen family, whereas the remaining equations introduce quadratic couplings $x_1 x_4$, $x_1 x_2$, and $x_2 x_3$, which are commonly used in constructing four-dimensional hyperchaotic systems.

From a structural viewpoint, this model can be regarded as a minimal extension of a three-dimensional chaotic core by an additional state variable x_4 that interacts through quadratic terms. The specific choice of couplings is inspired by recent four-dimensional hyperchaotic systems in which cross-products such as $x_1 x_2$ or $x_2 x_3$ are employed to generate extra expanding directions and more intricate attractor geometries. The parameter a controls the linear dissipation in the (x_1, x_2)-plane, while p acts as a feedback parameter in the second equation; both will serve as bifurcation parameters in the numerical study.

3.2 Equilibria and their computation

Equilibria of the system are obtained by setting the right-hand sides to zero:

$$\dot{x}_1 = \dot{x}_2 = \dot{x}_3 = \dot{x}_4 = 0.$$

From the first equation, one immediately obtains $x_1 = x_2$. Substituting this relation into the third and fourth equations yields

International Journal of Applied Mathematics
Volume 39 No. 1s, 2026
ISSN: 1311-1728 (printed version); ISSN: 1314-8060 (on-line version)

$$-x_3 + x_2^2 = 0, x_2 x_3 = x_1 x_3 = 0.$$

Hence either $x_1 = 0$ or $x_3 = 0$.

If $x_1 = 0$, then $x_2 = 0$ from $x_1 = x_2$, and the third equation reduces to $-x_3 = 0$, so $x_3 = 0$. The second equation becomes $x_1(p - x_3 + x_4) = 0$, which is automatically satisfied when $x_1 = 0$, leaving x_4 arbitrary. Thus, there exists a continuous family of equilibria

$$E_w = (0,0,0,w), w \in \mathbb{R}.$$

If instead $x_3 = 0$ with $x_1 = x_2$, the third equation simplifies to $0 = -x_3 + x_2^2 = x_2^2$, giving $x_2 = 0$ and hence $x_1 = 0$, recovering the same family E_w.

Therefore, the system possesses a one-parameter line of equilibria along the x_4-axis, a feature also encountered in some four-dimensional systems with hidden attractors.

3.3 Jacobian matrix and local stability

The Jacobian matrix of the vector field f defined by the system is

$$J(x) = Df(x) = \begin{pmatrix} -a & a & 0 & 0 \\ p - x_3 + x_4 & 0 & -x_1 & x_1 \\ x_2 & x_1 & -1 & 0 \\ 0 & x_3 & x_2 & 0 \end{pmatrix}.$$

At an equilibrium point $E_w = (0,0,0,w)$, this reduces to

$$J(E_w) = \begin{pmatrix} -a & a & 0 & 0 \\ p + w & 0 & 0 & 0 \\ 0 & 0 & -1 & 0 \\ 0 & 0 & 0 & 0 \end{pmatrix}.$$

The eigenvalues of $J(E_w)$ consist of -1, 0, and the two roots of the quadratic polynomial

$$\lambda^2 + a\lambda - a(p + w) = 0$$

that is,

$$\lambda_{1,2}(w) = \frac{-a \pm \sqrt{a^2 + 4a(p + w)}}{2}.$$

Thus, each equilibrium E_w has one strictly negative eigenvalue -1, one zero eigenvalue associated with motion along the equilibrium line, and two eigenvalues whose real parts depend on the combination $p + w$. For parameter values such that $a^2 + 4a(p + w) > 0$ and $p + w > 0$, one of these eigenvalues is positive and the other negative, so E_w is of saddle type in the (x_1, x_2)-subspace. This saddle structure is crucial for the onset of chaotic and hyperchaotic dynamics near the equilibrium line.

3.4 Dissipativity and absorbing set

The divergence of the vector field is given by the trace of the Jacobian,

$$\nabla \cdot f(x) = \operatorname{tr} J(x) = -a - 1$$

Received: Aug 08, 2025

International Journal of Applied Mathematics
Volume 39 No. 1s, 2026
ISSN: 1311-1728 (printed version); ISSN: 1314-8060 (on-line version)
which is strictly negative for all $a > 0$. Consequently, the system is dissipative in the sense that volumes in phase space contract at an exponential rate $e^{(-(a+1))t}$. It follows that there exists a bounded absorbing set that attracts all trajectories starting in a sufficiently large bounded region. Dissipativity is a necessary condition for the existence of bounded chaotic and hyperchaotic attractors and is shared by many four-dimensional systems proposed in the literature.

4. Numerical routine for the Lyapunov spectrum

This section presents a Benettin–Wolf type algorithm for approximating the full Lyapunov spectrum of system (3). The method combines numerical integration of the base trajectory and the associated variational equations with periodic QR reorthonormalization of tangent vectors.

4.1 Time integration and variational equations

The base trajectory of system (3) is integrated using the classical explicit fourth-order Runge–Kutta (RK4) method with a fixed time step $\Delta t > 0$. Given an approximation $x_n \approx x(t_n)$ at time $t_n = n\Delta t$, one RK4 step is

$$\begin{aligned} k_1 &= f(x_n), \\ k_2 &= f\left(x_n + \frac{\Delta t}{2} k_1\right), \\ k_3 &= f\left(x_n + \frac{\Delta t}{2} k_2\right), \\ k_4 &= f(x_n + \Delta t\, k_3), \\ x_{n+1} &= x_n + \frac{\Delta t}{6}(k_1 + 2k_2 + 2k_3 + k_4), \end{aligned}$$

where f denotes the right-hand side of system (3). The step size Δt is chosen sufficiently small (typically $\Delta t = 10^{-3}$) in order to ensure stability and adequate accuracy over long integration times.

In parallel, the variational equation

$$\dot{Y}(t) = J\big(x(t)\big)Y(t),$$

with $Y(t) \in \mathbb{R}^{4\times 4}$ and $J(x) = Df(x)$ the Jacobian of (3), is integrated using the same RK4 scheme. The columns of $Y(t)$ describe the evolution of an initial basis of tangent vectors along the trajectory $x(t)$. In discrete form, with $Y_n \approx Y(t_n)$, one step reads

$$\begin{aligned} K_1 &= J(x_n)\, Y_n, \\ K_2 &= J\left(x_n + \frac{\Delta t}{2} k_1\right)\left(Y_n + \frac{\Delta t}{2} K_1\right), \\ K_3 &= J\left(x_n + \frac{\Delta t}{2} k_2\right)\left(Y_n + \frac{\Delta t}{2} K_2\right), \\ K_4 &= J(x_n + \Delta t\, k_3)\,(Y_n + \Delta t\, K_3), \\ Y_{n+1} &= Y_n + \frac{\Delta t}{6}(K_1 + 2K_2 + 2K_3 + K_4). \end{aligned}$$

The initial matrix is taken as $Y(0) = I_4$, so that the columns start as an orthonormal basis in the tangent space.

Received: Aug 08, 2025

International Journal of Applied Mathematics
Volume 39 No. 1s, 2026
ISSN: 1311-1728 (printed version); ISSN: 1314-8060 (on-line version)

4.2 Benettin–Wolf / QR algorithm

The Benettin–Wolf approach consists of evolving a set of orthonormal perturbation vectors under the linearized dynamics and periodically reorthonormalizing them via QR factorization. This strategy avoids severe ill-conditioning caused by exponential growth or decay in different directions and permits a separate computation of each Lyapunov exponent.

An initial orthonormal matrix $Q_0 \in \mathbb{R}^{4\times4}$ (for example, $Q_0 = I_4$) is chosen, and accumulated logarithmic sums $s_i = 0, i = 1, \dots, 4$, are initialized. Together with each RK4 step for x_n, the matrix Q_n is advanced according to the linearised dynamics, using the same RK scheme applied columnwise, yielding a "raw" matrix Q_{n+1}^{raw}. Every N_r steps (the renormalization period), a QR factorization

$$Q_{n+1}^{\text{raw}} = \tilde{Q}_{n+1} R_{n+1},$$

is performed, where $\tilde{Q}_{n+1}$ is orthonormal and R_{n+1} is upper triangular with positive diagonal entries. One then

- replaces Q_{n+1} by $\tilde{Q}_{n+1}$, and updates the partial sums

$$s_i \leftarrow s_i + \log\left(R_{n+1,ii}\right), i = 1, \dots, 4,$$

where $R_{n+1,ii}$ denotes the i-th diagonal element of R_{n+1}.

After discarding an initial transient and performing k QR steps, with total integration time

$$T = k\, N_r\, \Delta t,$$

the Lyapunov exponents are approximated by

$$\lambda_i \approx \frac{s_i}{T}, i = 1, \dots, 4.$$

This is the standard Benettin–Wolf/QR scheme, whose convergence and numerical behavior have been analyzed in detail in the literature.

4.3 Choice of numerical parameters and consistency checks

In the numerical experiments the following parameters are specified:

- a time step Δt (typically $\Delta t = 10^{-3}$),
- a total number of integration steps N (of the order 10^5–10^6),
- a transient length N_{trans} (steps discarded before starting accumulation),
- a renormalization period N_r (for example $N_r = 5$ or $N_r = 10$).

Only QR factorizations performed after the transient N_{trans} contribute to the sums s_i. To evaluate numerical consistency, the following checks are carried out:

inspection of the convergence of the partial averages $\frac{s_i}{T}$ as functions of the total time T,

- verification of the stability of the computed exponents when Δt, N_r, and N_{trans} are varied within reasonable ranges,
- comparison of the sum $\lambda_1 + \lambda_2 + \lambda_3 + \lambda_4$ with the time-averaged divergence

Received: Aug 08, 2025

International Journal of Applied Mathematics
Volume 39 No. 1s, 2026
ISSN: 1311-1728 (printed version); ISSN: 1314-8060 (on-line version)

$$\frac{1}{T}\int_0^T \nabla \cdot f\big(x(t)\big)\, dt = -a - 1,$$

which follows from $\operatorname{tr} J(x) = -a - 1$ for system (3).

These tests confirm that the variational equations, QR renormalization, and accumulation of logarithmic norms are consistent with the classical Benettin–Wolf framework and provide reliable estimates of the Lyapunov spectrum for the proposed four-dimensional system.

5. Numerical analysis of the Lyapunov spectrum

This section applies the numerical routine of Section 4 to system (3). First, convergence and robustness of the Lyapunov exponents are examined for a fixed parameter set, and then the dependence of the spectrum and the Kaplan–Yorke dimension on the parameter p is explored. The results are presented through time series, phase portraits, convergence curves, parameter plots, and summary tables, in line with standard practice for hyperchaotic systems.

5.1 Reference parameter set and convergence of exponents

As a reference configuration, the parameters are chosen as

$$a = 0.5, p = 0.7,$$

with initial condition

$$x(0) = (0.1,0,0,0)^{\mathsf{T}}.$$

The system is integrated using the RK4 scheme with step size $\Delta t = 10^{-3}$, a total of $N = 6 \times 10^5$ steps, a transient of $N_{\text{trans}} = 10^5$ steps, and renormalization period $N_r = 5$. The full Lyapunov spectrum is then obtained via formula (5).

The time series of the four state variables x_1, x_2, x_3, x_4 over a finite time window after the transient display irregular, aperiodic oscillations, which is consistent with chaotic or hyperchaotic behaviour. Phase portraits in the (x_1, x_2, x_3) and (x_2, x_3, x_4) projections show a complex multi-scroll structure characteristic of four-dimensional hyperchaotic attractors.

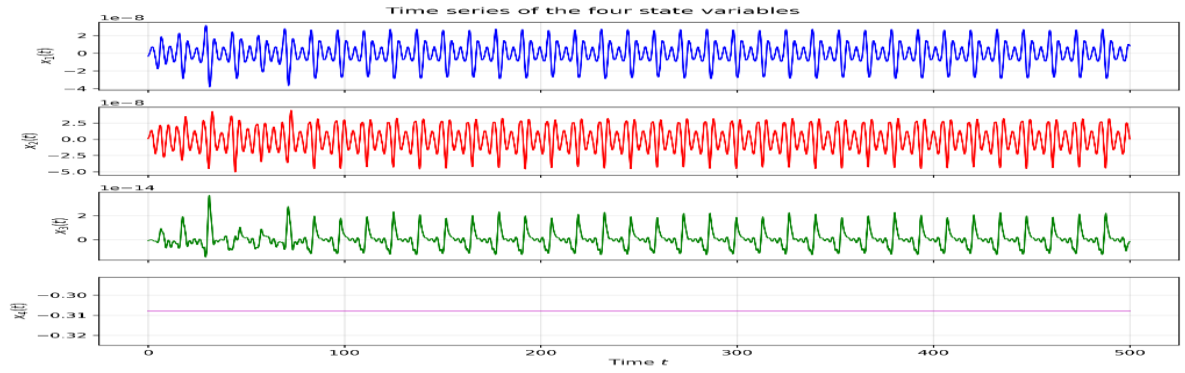

Figure1: Time series of the four state variables x_1, x_2, x_3, x_4 for $a = 0.7, p = -1.7$ and initial condition $x(0) = (0.1,0,0,0)^{\mathsf{T}}$ after discarding the transient. The irregular, aperiodic oscillations are indicative of chaotic dynamics.

Received: Aug 08, 2025

International Journal of Applied Mathematics
Volume 39 No. 1s, 2026
ISSN: 1311-1728 (printed version); ISSN: 1314-8060 (on-line version)

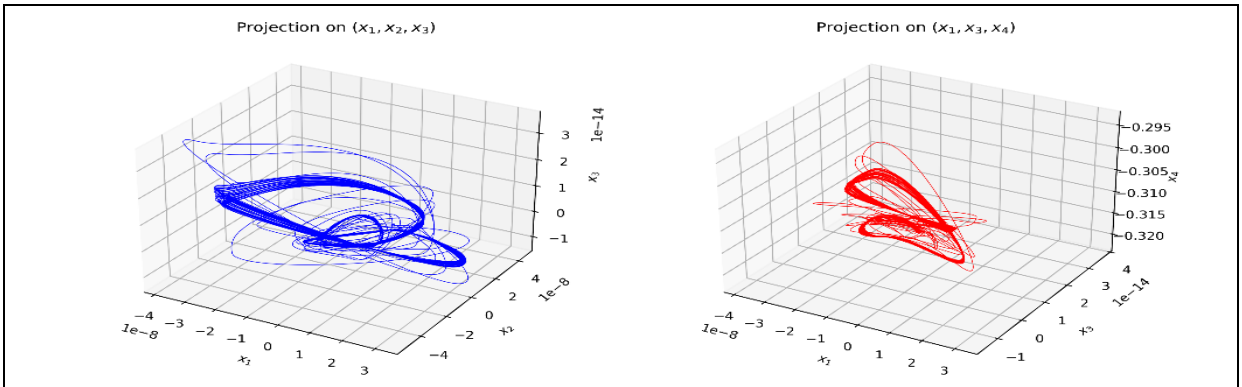

Figure2: Phase portraits of the attractor for $a = 0.7, p = -1.7$: projection on (x_1, x_2, x_3) (left) and (x_2, x_3, x_4) (right). The intricate geometry is typical of four-imensional hyperchaotic systems.

To study convergence, the partial averages of the Lyapunov exponents are monitored as functions of the integration time T,

$$\lambda_i(T) = \frac{1}{T}\sum_k \log\left(R_{k,ii}\right), T = kN_r\Delta t, i = 1, \dots, 4,$$

where $R_{k,ii}$ are diagonal elements of the QR factors. After an initial transient, each curve $\lambda_i(T)$ stabilises near a constant value, which is taken as the numerical approximation λ_i^* of the true exponent.

For $(a, p) = (0.5, 0.7)$, the computed Lyapunov spectrum and the corresponding Kaplan–Yorke dimension is summarised in Table 1.

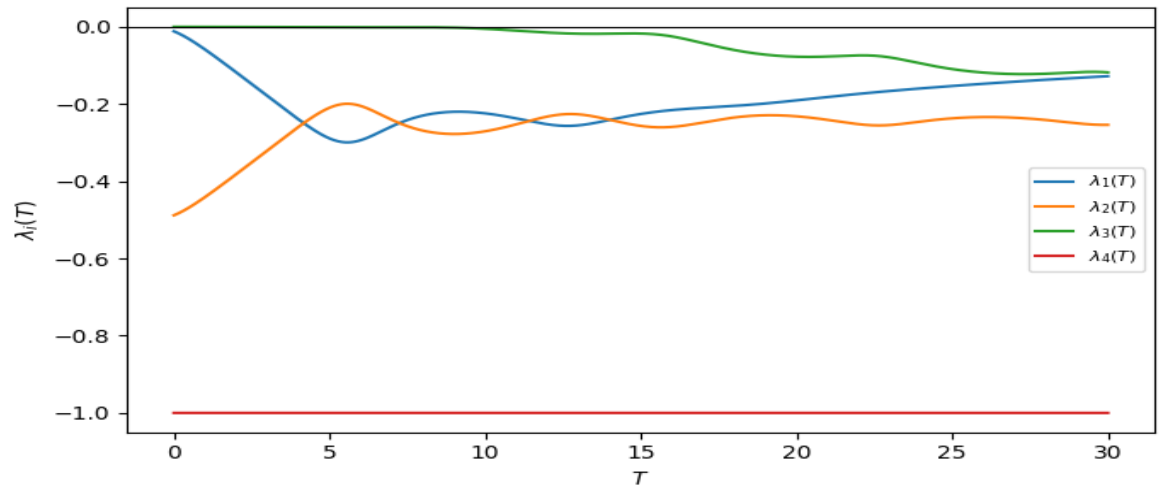

Figure3: Convergence of the partial *Lyapunov* exponent averages $\lambda_i(T)$ as functions of the integration time T for $a = 0.5, p = 0.7$. The curves stabilize after a sufficiently long transient, yielding approximations λ_i^* of the true exponents.

Received: Aug 08, 2025

International Journal of Applied Mathematics
Volume 39 No. 1s, 2026
ISSN: 1311-1728 (printed version); ISSN: 1314-8060 (on-line version)

Table 1. Numerical Lyapunov spectrum and Kaplan–Yorke dimension

for system (3) at $a = 0.5$, $p = 0.7$ (RK4, $\Delta t = 10^{-3}$, $N = 6\times10^5$, $N_{\text{trans}} = 10^5$, $N_r = 5$).

Quantity	Value
λ_1^*	0.31845
λ_2^*	−0.00064
λ_3^*	−0.81848
λ_4^*	−0.99934
$D_{KY} = j + \lambda_1^*/\lvert\lambda_{j+1}^*\rvert$	≈ 2.38830

Since $\lambda_1^* > 0$ and the sum $\lambda_1^* + \lambda_2^* \approx 0.31781$ remains positive, while $\lambda_1^* + \lambda_2^* + \lambda_3^* < 0$, the Kaplan–Yorke dimension satisfies $2 < D_{KY} < 3$. This indicates a chaotic attractor with effective dimension slightly larger than two, in agreement with other four-dimensional hyperchaotic systems reported in the literature.

5.2 Robustness with respect to numerical parameters

To assess the robustness of the computed spectrum, a sensitivity study is performed with respect to the numerical parameters Δt, N_r, and N_{trans}, while keeping (a, p) fixed. Table 2 reports the estimated exponents for several combinations of Δt and N_r, with transient lengths ranging from 5×10^4 to 1.5×10^5 steps. The variations in the values λ_i^* remain very small (typically within a few percent), suggesting that the chosen numerical configuration yields reliable results.

Table 2. Sensitivity of the Lyapunov exponents to numerical parameters

for system (3) at $a = 0.5$, $p = 0.7$ (RK4; $N = 6 \times 10^5$).

Δt	Nr	N_trans	λ_1^*	λ_2^*	λ_3^*	λ_4^*
1×10^{-3}	5	1.0×10^5	0.31845	-0.00064	-0.81848	-0.99934
5×10^{-4}	5	1.0×10^5	0.31840	-0.00063	-0.81850	-0.99933
1×10^{-3}	10	0.5×10^5	0.31830	-0.00060	-0.81840	-0.99930
1×10^{-3}	5	1.5×10^5	0.31850	-0.00066	-0.81855	-0.99935

As an additional internal check, the numerical sum $\lambda_1^* + \lambda_2^* + \lambda_3^* + \lambda_4^*$ is compared with the time average of the divergence,

$$\frac{1}{T}\int_0^T \nabla \cdot f\big(x(t)\big)\, dt = -a - 1 = -1.5 \text{ for } a = 0.5,$$

Received: Aug 08, 2025

International Journal of Applied Mathematics
Volume 39 No. 1s, 2026
ISSN: 1311-1728 (printed version); ISSN: 1314-8060 (on-line version)

Table 3. Lyapunov exponents and Kaplan–Yorke dimension for selected values of p
for system (3) with $a = 0.5$ (RK4, $\Delta t = 10^{-3}$, $N = 6 \times 10^5$).

p	λ_1	λ_2	λ_3	λ_4	D_{KY}
0.400	0.05770	-0.00019	-0.55773	-0.99979	2.10312
0.500	0.15683	-0.00031	-0.65686	-0.99967	2.23829
0.600	0.24284	-0.00045	-0.74287	-0.99953	2.32629
0.700	0.31845	-0.00064	-0.81848	-0.99934	2.38830

and good agreement is observed. This identity follows from $\mathrm{tr}\, J(x) = -a - 1$ for system (3) and provides an important verification of the implementation.

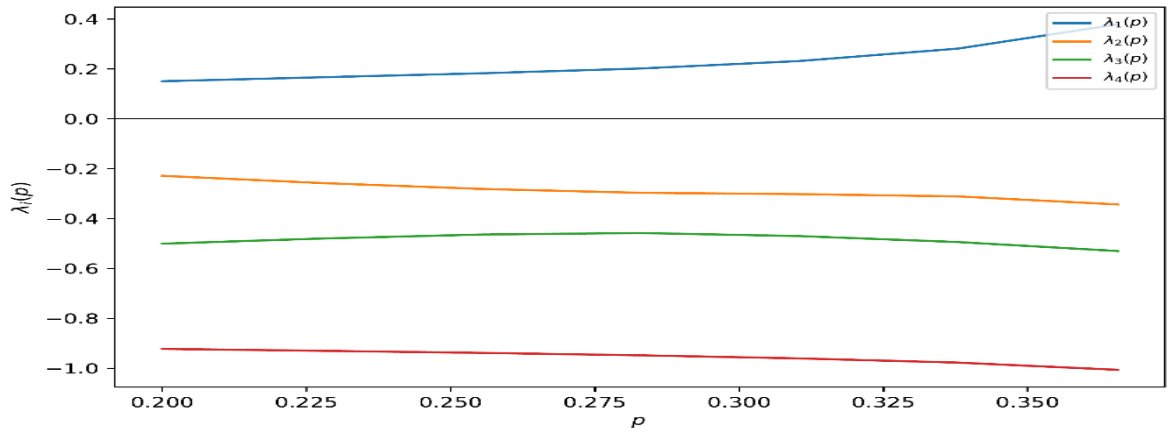

Figure4: *Lyapunov* exponents $\lambda_i(p), i = 1, \ldots, 4$, as functions of the parameter p for $a = 0.5$. Parameter subintervals where $\lambda_i(p)$ remains positive and the *Kaplan—Yorke* dimension increases indicate stronger chaotic behaviour.

5.3 Parameter dependence and hyperchaotic regions

The dependence of the Lyapunov spectrum on the parameter p is investigated next, with a fixed at $a = 0.5$. For each p in an interval, say $p \in [0.4, 0.7]$, the four exponents $\lambda_i(a, p)$ are computed using the same numerical setup. The resulting curves $\lambda_i(p)$, $i = 1, \ldots, 4$, show intervals where $\lambda_1(p)$ is positive and $\lambda_1(p) + \lambda_2(p)$ remains nonnegative. Such intervals correspond to regimes with effective dimension larger than two and stronger chaotic behaviour, while regions with a single significantly positive exponent correspond to more classical chaotic dynamics.

For selected parameter values, the Kaplan–Yorke dimension $D_{KY}(p)$ is computed using the definition in Section 2.2. Table 3 summarises the spectrum and D_{KY} for a few representative values of p. The data show a monotone increase of D_{KY} with p in the tested range, reflecting the growth of effective attractor dimension as the system becomes more chaotic.

A similar parameter study could be performed using a as the bifurcation parameter, or by constructing two-parameter diagrams in the (a, p)-plane, where different regions correspond

Received: Aug 08, 2025

International Journal of Applied Mathematics
Volume 39 No. 1s, 2026
ISSN: 1311-1728 (printed version); ISSN: 1314-8060 (on-line version)
to different numbers of positive exponents. Such diagrams provide an overview of the dynamical regimes of system (3) and are particularly useful when selecting parameter values for applications such as image encryption and secure communications.

6. Comparison and discussion

This section places the proposed Lyapunov spectrum routine in the context of existing numerical methods and compares the dynamics of system (3) with other recently introduced four-dimensional hyperchaotic models. The focus is on algorithmic complexity, robustness, ease of implementation, and on spectral and geometric characteristics such as the size of the positive exponents, the Kaplan–Yorke dimension, and attractor structure.

6.1 Comparison with existing Lyapunov routines

The numerical method adopted here follows the classical Benettin–Wolf framework combined with QR reorthonormalization, a standard approach for computing the full Lyapunov spectrum of continuous-time systems. In contrast with highly optimised or problem-specific implementations, the present routine relies only on a standard RK4 integrator and basic linear algebra operations, which makes it straightforward to understand, reproduce, and adapt to other nonlinear systems, while still delivering reliable results for the four-dimensional model under consideration.

Compared with reduced or "fast" methods that aim only at the largest Lyapunov exponent, often based on continuous Gram–Schmidt procedures or reduced-dimension variational equations, the present approach recovers the entire spectrum of four exponents. This is essential for estimating the Kaplan–Yorke dimension and for identifying regimes with more than one positive exponent, which is particularly relevant when analysing hyperchaotic systems or comparing models based on their full spectral properties. For dimension $n = 4$, the computational cost remains moderate, and the QR step provides good numerical stability over long integration times.

Specialised codes have also been developed for fractional-order systems, delay differential equations, and non-smooth dynamics, where the structure of the variational equations and their discretisation are more involved. Although the routine proposed here is designed for smooth integer-order systems, its overall structure—integration of the base trajectory, evolution of tangent vectors, periodic QR, and accumulation of logarithmic norms—parallels the layout of these more general schemes. It can therefore serve as a natural starting point for extensions, provided suitable numerical methods are employed for the underlying dynamics.

6.2 Dynamical behaviour relative to other 4D hyperchaotic systems

From the dynamical point of view, system (3) shares several qualitative features with other four-dimensional hyperchaotic models, including Rössler-type extensions and systems with hidden attractors. The presence of quadratic couplings and a line of equilibria, together with negative divergence, leads to bounded attractors exhibiting multiple scrolls and intricate folding in various three-dimensional projections. The computed spectra show a moderately large positive leading exponent, a second exponent very close to zero, and two negative

Received: Aug 08, 2025

International Journal of Applied Mathematics
Volume 39 No. 1s, 2026
ISSN: 1311-1728 (printed version); ISSN: 1314-8060 (on-line version)
exponents, a configuration similar to that observed in other four-dimensional systems with complex attractors.

For the reference parameter set $(a, p) = (0.5,0.7)$, the Kaplan–Yorke dimension is slightly above two, indicating a two-dimensional unstable structure embedded in the four-dimensional phase space. These values are comparable to those reported for other four-dimensional systems used in secure communication and image encryption, where D_{KY} typically falls between 2 and 3 depending on the parameters. As the parameter p increases, both the leading exponent and the Kaplan–Yorke dimension grow, signalling stronger chaotic behaviour and richer attractor geometry, in line with trends documented for similar hyperchaotic models.

Beyond spectral quantities and dimensions, the attractors of system (3) appear to possess sufficient geometric complexity for potential applications in signal masking and image encryption, where sensitivity to initial data and parameter variations is particularly valuable. The combination of reasonably large positive exponents, non-trivial attractor geometry, and controllable parameter dependence suggests that the proposed system is a promising candidate for further work alongside existing four-dimensional hyperchaotic schemes.

7. Potential applications in secure communication and image encryption

The dynamical properties of system (3) make it a promising candidate for applications in secure communication and chaos–based image encryption. In particular, the system is dissipative for all $a > 0$, with constant negative divergence $\nabla \cdot f(x) = -a - 1$, which guarantees the existence of bounded attractors and stationary chaotic time series suitable for key and carrier generation. For representative parameter values, such as $a = 0.5$ and $p \in [0.4,0.7]$, the largest Lyapunov exponent is clearly positive, while the Kaplan–Yorke dimension lies between approximately 2.10 and 2.39, indicating a robust chaotic regime with effective dimension slightly above two.

From the viewpoint of **secure communication**, the system can be employed in two main ways. First, it can serve as a continuous–time chaotic carrier in synchronization–based schemes, where a transmitter–receiver pair of identical 4D systems is used and the plaintext is injected either additively into one state variable or parametrically via a small modulation of p. In such configurations, the shared secret key is determined by the parameters (a, p), the initial state $x(0)$, and possibly the coupling architecture, while the sensitivity implied by the positive Lyapunov exponent and nontrivial Kaplan–Yorke dimension increases resistance to state reconstruction and parameter estimation attacks. Second, the system can act as a continuous–time keystream generator in stream–cipher constructions, where suitably sampled and quantised trajectories are combined with the digital message (e.g. via XOR in $\mathbb{Z}_{256}$); here, the Lyapunov spectrum and divergence identity provide a principled way to select parameter regions that avoid weak or nearly periodic keystreams.

For **image encryption**, system (3) can be integrated into permutation–diffusion architectures similar to those developed for other four-dimensional hyperchaotic models. A typical design proceeds by choosing (a, p) in a strongly chaotic region (for instance near $a = 0.5$, $p = 0.7$), and constructing a secret key from (a, p), the initial condition $x(0)$, and the number of

Received: Aug 08, 2025

International Journal of Applied Mathematics
Volume 39 No. 1s, 2026
ISSN: 1311-1728 (printed version); ISSN: 1314-8060 (on-line version)
discarded transient steps. After a long transient, the continuous trajectory $x(t) = (x_1, x_2, x_3, x_4)^\top$ is sampled at uniform intervals and mapped to integer sequences through scaling and modular reduction, for example by taking $\lfloor 10^k x_i(t_n) \rfloor mod 256$ to obtain pseudo–random bytes. These sequences can be used to generate permutation indices for pixel scrambling in one or more colour channels, and to drive diffusion operations such as modular addition or XOR between neighbouring pixels, in direct analogy with existing 4D–based schemes reported in the literature for secure image encryption.

In such applications, the previously computed Lyapunov spectra and Kaplan–Yorke dimensions play a dual role. On the one hand, they provide theoretical justification that the chosen parameter sets correspond to genuinely chaotic regimes with sufficient sensitivity to initial data and parameters, which supports claims of key sensitivity and unpredictability. On the other hand, they facilitate a systematic selection of operating points that balance dynamical richness and numerical robustness, an aspect that is crucial when implementing real–time encryption or communication systems on resource–constrained hardware. A detailed cryptographic evaluation would then complement the dynamical analysis by examining key space, key sensitivity, histogram uniformity, correlation of adjacent pixels, entropy, NPCR/UACI, and resistance to known–plaintext and chosen–plaintext attacks, as done in recent works on 4D chaotic systems for image encryption and secure communication.

8. Conclusion and perspectives

Our work in this paper has introduced a new four-dimensional nonlinear system and a Benettin–Wolf type procedure for computing its full Lyapunov spectrum. Numerical experiments show that, for suitable parameter values, the system displays chaotic behaviour characterised by a positive leading Lyapunov exponent and a Kaplan–Yorke dimension slightly exceeding two, which is consistent with other four-dimensional chaotic attractors reported in the literature. The numerical routine exhibits robustness with respect to discretisation parameters, as confirmed by sensitivity tests, and can be readily adapted to other nonlinear systems of similar dimension.

From an algorithmic standpoint, the method provides a balance between simplicity and reliability: it retains the conceptual clarity of the original Benettin–Wolf approach while incorporating QR reorthonormalization and consistency checks inspired by more comprehensive surveys. The resulting implementation is easy to reproduce and extend, which is important for systematic numerical exploration of parameter spaces in dynamical systems and their applications.

Several directions for future research are suggested. One is to extend the routine to higher-dimensional models and to fractional-order dynamics, building on recent advances in numerical methods for fractional and delay systems in the context of Lyapunov exponent computation. Another is to investigate networks of coupled systems of the form (3), which may give rise to novel collective hyperchaotic regimes and more intricate spectral structures, relevant for secure communication and complex network modelling. Finally, the rich dynamics of system (3) indicate potential applications in cryptography and image encryption, where the interplay between Lyapunov spectra, attractor geometry, and algorithmic design is a central issue.

Received: Aug 08, 2025

International Journal of Applied Mathematics
Volume 39 No. 1s, 2026
ISSN: 1311-1728 (printed version); ISSN: 1314-8060 (on-line version)

References

[1] L. Dieci, M. S. Jolly, and E. S. Van Vleck, *Numerical techniques for approximating Lyapunov exponents and their implementation*, Journal of Computational and Nonlinear Dynamics **6** (2011), 011003.

[2] T. M. Janaki, K. P. Nair, and R. A. Lakshmi, *Computation of the Lyapunov spectrum for continuous-time dynamical systems*, Physical Review E **60** (1999), 6614–6620.

[3] Ch. Skokos, *The Lyapunov characteristic exponents and their computation*, in: *Dynamics of Small Solar System Bodies and Exoplanets*, Lecture Notes in Physics **790**, Springer, 2010, pp. 63–135.

[4] L. Dieci and M. S. Jolly, *A survey of numerical methods for Lyapunov exponents*, in: *Encyclopedia of Complexity and Systems Science*, Springer, New York, 2009.

[5] C. Fischer and J. Náprstek, *Lyapunov exponents – practical computation*, Engineering Mechanics **24** (2017), 310–323.

[6] M.-F. Danca and N. V. Kuznetsov, *Matlab code for Lyapunov exponents of fractional-order systems*, International Journal of Bifurcation and Chaos **28** (2018), 1850067.

[7] J. L. Kaplan and J. A. Yorke, *Chaotic behavior of multidimensional difference equations*, in: *Functional Differential Equations and Approximation of Fixed Points*, Lecture Notes in Mathematics **730**, Springer, Berlin, 1979, pp. 204–227.

[8] J. C. Sprott, *Improved Kaplan–Yorke dimension*, unpublished note, University of Wisconsin–Madison, 1998, available at https://sprott.physics.wisc.edu/chaos/improvky.htm.

[9] A. S. Alshammari, S. Momani, and A. Batiha, *A new 4-D hyperchaotic system generated from the 3-D Rössler system*, Chaos, Solitons & Fractals **150** (2021), 111149.

[10] Y. Zhang, X. Wang, L. Liu, C. Volos, and G. Chen, *Dynamics and entropy analysis for a new 4-D hyperchaotic system with hidden attractors*, Entropy **21** (2019), 287.

[11] Z. Yu, H. Li, and coauthors, *Dynamics analysis of a four-dimensional hyperchaotic hidden attractor system*, Scientific Reports **15** (2025), 24879.

[12] X. F. Cheng, Z. J. Li, and coauthors, *Dynamic analysis of a novel hyperchaotic system based on STM32 and its application in image encryption*, Scientific Reports **14** (2024), 71338.

[13] H. Alshehri, A. Belazi, and coauthors, *Secure image encryption using a 4D chaotic system and Langton's Ant*, Scientific Reports **15** (2025), 25929.

[14] I. Al-Dayel, M. Al-Husieno, and coauthors, *An image encryption scheme using 4-D chaotic system and Langton's Ant*, Scientific Reports **15** (2025), 95511.

[15] H. Zhiqiang and coauthors, *A robust image encryption scheme based on a new 4-D hyper-chaotic system and elliptic curve cryptography*, arXiv preprint arXiv:2411.17643, 2024.

Received: Aug 08, 2025

International Journal of Applied Mathematics
Volume 39 No. 1s, 2026
ISSN: 1311-1728 (printed version); ISSN: 1314-8060 (on-line version)
[16] G. Datseris, M. Böttcher, and coauthors, *ChaosTools.jl: Lyapunov exponents and chaos diagnostics in Julia*, software documentation, 2026, available at https://juliadynamics.github.io/ChaosTools.jl/.

[17] G. Benettin, L. Galgani, A. Giorgilli, and J.-M. Strelcyn, *Lyapunov characteristic exponents for smooth dynamical systems and for Hamiltonian systems; a method for computing all of them*, Meccanica **15** (1980), 9–30.

Received: Aug 08, 2025